Namwoo Kang[1]
Mem. ASME
Optimal Design Laboratory,
Department of Mechanical Engineering,
University of Michigan,
Ann Arbor, MI 48109
e-mail: nwkang@umich.edu

Fred M. Feinberg
Professor
Ross School of Business,
University of Michigan,
Ann Arbor, MI 48109
e-mail: feinf@umich.edu

Panos Y. Papalambros
Professor
Fellow ASME
Optimal Design Laboratory,
Department of Mechanical Engineering,
University of Michigan,
Ann Arbor, MI 48109
e-mail: pyp@umich.edu

Integrated Decision Making in Electric Vehicle and Charging Station Location Network Design

A major barrier in consumer adoption of electric vehicles (EVs) is "range anxiety," the concern that the vehicle will run out of power at an inopportune time. Range anxiety is caused by the current relatively low electric-only operational range and sparse public charging station (CS) infrastructure. Range anxiety may be significantly mitigated if EV manufacturers and CS operators work in partnership using a cooperative business model to balance EV performance and CS coverage. This model is in contrast to a sequential decision-making model where manufacturers bring new EVs to the market first and CS operators decide on CS deployment given EV specifications and market demand. This paper proposes an integrated decision-making framework to assess profitability of a cooperative business model using a multidisciplinary optimization model that combines marketing, engineering, and operations considerations. This model is demonstrated in a case study involving battery EV design and direct current (DC) fast-CS location network in Southeast Michigan. The expected benefits can motive both government and private enterprise actions. [DOI: 10.1115/1.4029894]

1 Introduction

In the EV market, one can identify five key players besides the consumers themselves [1]: original equipment manufacturers (OEMs) assemble vehicles and sell them to consumers; battery manufacturers supply batteries to OEMs; utilities supply electricity to CSs; CS manufacturers supply EV supply equipment (EVSE) to utilities; and governments support all related activities through a variety of policies.

EVs face several consumer adoption barriers such as vehicle operating range, vehicle cost, perceived safety, unusual emergency situations, reliability, vehicle size and performance, infrastructure support, long charging time, high charging cost, and long payback period expectations [1,2]. The individual market players mentioned above are expending significant effort to overcome such barriers. In this paper, we adopt the argument that to overcome these barriers effectively, the market players must use a holistic approach to develop cooperatively integrated business models rather than just pursue their individual business models [3]. In this spirit, we present a mathematical formulation of a decision-making (optimization) framework that can support an integrated business model. Some of the market players are already cooperating in the market using business to business (B2B) models. For example, cooperation of OEMs and battery manufacturers or cooperation of utilities and CS manufacturers is common. In the current study, we address a cooperative business model between two groups: EV manufacturers (i.e., OEMs and battery manufacturers) and CS operators (i.e., utilities and CS manufacturers).

A major barrier to consumer adoption is *range anxiety*. The consumer perception of its importance depends not only on the actual operating range determined by the design of the vehicle and its battery (versus that of a conventional fuel vehicle) but also on the availability of CSs and required charging times when the consumer plans a particular, possibly long, trip. Thus, consumers hesitate to buy EVs due to range anxiety, EV manufacturers hesitate to develop and produce EVs due to small market demand, and CS operators hesitate to invest in charging infrastructure for the same reason [4].

Addressing range anxiety requires coordination of engineering business decisions by EV manufacturers and operation business decisions by CS operators. For example, a short range vehicle in a market with ample CSs may induce less range anxiety than a long range vehicle in a market with sparse CSs. Interestingly, research shows that the average daily driving range in the U.S. is less than 20 miles [5,6], and so range anxiety may be due more to a psychological need for security in an occasional long trip. Appealing to consumers through, say, joint advertising, for both EV performance and public CSs coverage as a "bundle" could be more effective in EV technology adoption. This approach could also address the issue of high initial vehicle cost due to a large battery pack that accounts for almost half of total consumer vehicle cost [7].

EV manufacturers and CS operators can partner to identify optimal "system" balance between vehicle performance and CS infrastructure to maximize market share or profit for both parties. A cooperative example in the U.S. is the EV project supported by the U.S. Department of Energy engaging partners such as ECOtality, Nissan LEAF, and Chevrolet Volt in major states [8]; the ChargePoint program supported by Coulomb Technologies is a cooperation among Chevrolet, Ford, and Smart USA [9]; Reliant Energy is working with Nissan in Houston, and Southern California Edison is working with Ford in CA. Such cooperations typically focus only on funding for installation of EVSEs in target EV markets rather than the broader cooperation suggested here.

In this study, we consider an independent CS operator (not state affiliated). The charging infrastructure consists of DC fast-CSs for commuting between major cities or trips longer than the range offered by a typical EV in the current market. EVs generally use three types of charging modes (or stations), level 1, level 2, and DC fast. It takes at least 3 hr to recharge a battery using levels 1 or 2, while DC fast can recharge a battery to 80% capacity (for safety reasons) within 30 min. DC fast-CSs are considered promising for a future public charging infrastructure, but there were only 154 stations in the U.S. as of 2012 [10].

The proposed decision-making framework combines the EV design and CS location network design problems. EV manufactures decide on vehicle price and attributes such as range, MPGe (miles per gallon gasoline equivalent), top-speed, and acceleration

[1]Corresponding author.

Contributed by the Design Automation Committee of ASME for publication in the Journal of Mechanical Design. Manuscript received September 24, 2014; final manuscript received February 16, 2015; published online March 30, 2015. Assoc. Editor: Gary Wang.

(0–60 mph). CS operators decide on charging fee, how many stations to build, and where these stations should be located considering EV range offered by the manufacturer. The optimization objective is to maximize overall profit, and it is assumed that EV manufacturers and CS operators invest together and share the profits. Optimization results show that a cooperative business model (i.e., integrated decision-making for overall profit) is more profitable than a sequential business model (i.e., engineering decision-making and then operating decision-making for maximizing each player's profit) for both partners.

The remainder of the paper is organized as follows. Section 2 introduces the decision-making framework and associated models. Section 3 presents an implementation case study for an EV market in Southeast Michigan. Sections 4 and 5 discuss results, conclusions, and limitations.

2 Integrated Decision-Making Framework

2.1 Framework. The decision-making framework consists of three models for marketing, engineering, and operations with shared decision variables. The framework is given in Fig. 1.

The EV design model represents the engineering problem with EV design variables ($\mathbf{x}_{EV}$) such as battery ($\mathbf{B}_{EV}$), motor ($\mathbf{M}_{EV}$), and gear (G_{EV}) designs as variable inputs; and EV attributes ($\mathbf{A}_{EV}$) such as range (r_{EV}), MPGe (mpg_{EV}), top-speed (sp_{EV}), and acceleration (acc_{EV}) as outputs. These outputs are used as inputs to the marketing and operations models.

The DC fast-CS location network model represents the operations problem with CS design variables ($\mathbf{x}_{CS}$) such as number (N_{CS}) and locations ($\mathbf{L}_{CS}$) of stations as variable inputs, EV range (r_{EV}) as input from engineering, and CS coverage ($\mathbf{CV}_{CS}$) as the output. This output is used as input to the marketing model. Coverage is defined as the percentage of possible paths a consumer can drive from the origin (e.g., home) without running out of power by using DC fast-CSs.

The marketing model predicts EV and CS demands (q_{EV}, q_{CS}) using the EV attributes ($\mathbf{A}_{EV}$) from the engineering model and CS coverage ($\mathbf{CV}_{CS}$) from the operations model as inputs, as well as EV price (p_{EV}) and charging fee (p_{CS}) as variable inputs.

The optimization objective is to maximize overall profit ($\Pi_{EV} + \Pi_{CS}$) from EVs and CSs with respect to the variables: EV price (p_{EV}), charging fee (p_{CS}), EV design ($\mathbf{x}_{EV}$), and CS design ($\mathbf{x}_{CS}$).

The overall optimization equation is stated as follows:

$$\max_{\bar{\mathbf{x}}} \quad \Pi_{EV} + \Pi_{CS} = (p_{EV} - c_{EV})q_{EV} + (p_{CS} - c_{EC})q_{CS} - c_{CS} \tag{1}$$

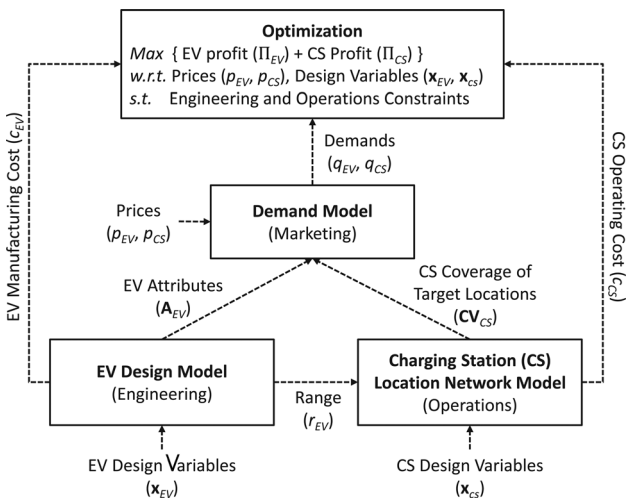

Fig. 1 Framework of decision-making

with respect to

$$\bar{\mathbf{x}} = [p_{EV}, p_{CS}, \mathbf{x}_{EV}, \mathbf{x}_{CS}]$$
$$\mathbf{x}_{EV} = [\mathbf{B}_{EV}, \mathbf{M}_{EV}, G_{EV}] \tag{2}$$
$$\mathbf{x}_{CS} = [N_{CS}, \mathbf{L}_{CS}]$$

subject to

$$lb \le \bar{\mathbf{x}} \le ub \tag{3}$$
$$\mathbf{g}(\mathbf{A}_{EV}) \le 0 \tag{4}$$

where

$$\mathbf{A}_{EV} = [r_{EV}, \text{mpg}_{EV}, \text{sp}_{EV}, \text{acc}_{EV}] \tag{5}$$

$$[c_{EV}, c_{CS}] = f_c(\mathbf{x}_{EV}, \mathbf{x}_{CS}) \tag{6}$$

$$[q_{EV}, q_{CS}] = f_q(p_{EV}, p_{CS}, \mathbf{A}_{EV}, \mathbf{CV}_{CS}) \tag{7}$$

$$\mathbf{A}_{EV} = f_{EV}(\mathbf{x}_{EV}) \tag{8}$$
$$\mathbf{CV}_{CS} = f_{CS}(\mathbf{x}_{CS}, r_{EV}) \tag{9}$$

where $\bar{\mathbf{x}}$ in Eq. (2) is decision variables, Eq. (3) is boundary constraints, and Eq. (4) is inequality constraints for EV attributes as shown in Table 2. Furthermore, f_c, f_q, f_{EV}, and f_{CS} are linking cost, demand, engineering, and operations outputs to decision variables, respectively. Each model is explained in more detail in Secs. 2.2, 2.3, and 2.4.

2.2 EV Design Model (Engineering). The engineering performance model of a battery EV (B_{EV}), f_{EV}, in Eq. (8) is built using the AMESIM software. The subsystem models include analytical expressions from the AMESIM libraries [11]. Previous research showed that analytical models of EV systems are appropriate for efficient system-level simulations in the early design stage, and their adequate fidelity has been assured through comparison with finite element models or laboratory measurements [12–14].

The engineering model here consists of driver, control unit, motor torque control, battery, inverter, permanent magnet synchronous motor, and vehicle models as shown in Fig. 2.

The overall architecture and vehicle parameters for the modeled vehicle are similar to the Nissan Leaf. The subsystems designed in the study are lithium-ion battery, permanent magnet synchronous motor, and gearing. Seven design variables and their lower and upper bounds are summarized in Table 1. Four responses (attributes) and associated inequality constraints are summarized in Table 2. These practical inequality constraints are placed to ensure highway driving feasibility.

2.2.1 Battery Design. We use the simple battery model shown in Fig. 3 where OCV is open circuit voltage, r is internal resistance, I is current, CF is filtering capacitance, and U is the output voltage. Based on this model, state of charge (SOC), output voltage, and heat flow rate (i.e., thermal losses) are computed as outputs of the simulation.

Battery design variables are the number of cells in series in one branch and the number of branches in parallel, and they are used to calculate the following battery characteristics:

$$C_{bt} = C_{cell} \cdot n_p \tag{10}$$
$$\text{CF}_{bt} = \text{CF}_{cell} \cdot \frac{n_p}{n_s} \tag{11}$$
$$\text{OCV}_{bt} = \text{OCV}_{cell} \cdot n_s \tag{12}$$
$$r_{bt} = r_{cell} \cdot \frac{n_s}{n_p} \tag{13}$$

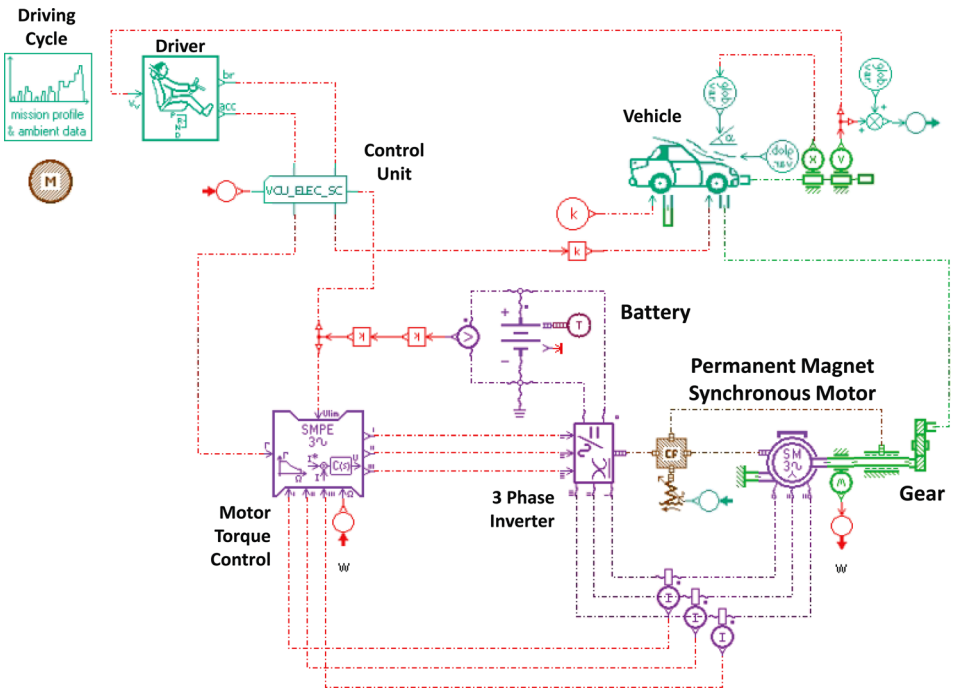

Fig. 2 Engineering simulation model

Table 1 Design variables of engineering model

System	Symbol	Design variables	Lower bound	Upper bound
Battery	n_s	Number of cells in series in one branch	80	200
	n_p	Number of branches in parallel	1	4
Motor	L_d	Stator inductance of the d-axis	1.62 mH	3.42 mH
	L_q	Stator inductance of the q-axis	1.98 mH	4.18 mH
	R_s	Stator resistance	0.001 Ω	0.1 Ω
	p	Number of pole pairs	1	4
Gear	G	Gear ratio	2	12

Table 2 Responses and inequality constraints of engineering model

Response	Constraint
Top-speed (sp_{EV})	≥70 mph
Acceleration (0–60 mph) (acc_{EV})	≤30 s
Range (r_{EV})	N/A
MPGe (mpg_{EV})	N/A

Here, n_s and n_p are the number of cells in series in one branch and the number of branches in parallel, respectively; C_{bt} is battery capacity, C_{cell} is cell capacity, CF_{bt} is battery filtering capacitance, CF_{cell} is cell filtering capacitance, OCV_{bt} is battery open circuit voltage, OCV_{cell} is cell open circuit voltage, r_{bt} is battery internal resistance, and r_{cell} is cell internal resistance. Since OCV_{cell} and r_{cell} are affected by SOC, OCV_{cell} and r_{cell} are computed by linear interpolation of available experimental data. All parameter values in the above equations are based on Nissan Leaf battery cell tests [15].

From the battery characteristics above, SOC, output voltage, and heat flow rate are computed

$$\frac{dSOC}{dt} = 100 \cdot \frac{I_2}{C_{bt}} \tag{14}$$

$$\frac{dU}{dt} = \frac{I_2 - \frac{U - OCV_{bt}}{r_{bt}}}{CF_{bt}} \tag{15}$$

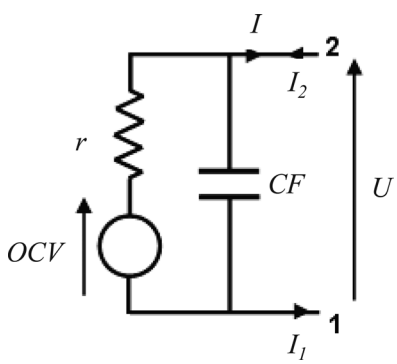

Fig. 3 Battery model [11]

$$dh = \frac{(U - OCV_{bt})^2}{r_{bt}} \tag{16}$$

where U is the output voltage and dh is heat flow rate based on Joule's losses.

2.2.2 Motor Design. The motor model outputs, such as torque and heat flow rate, are computed using permanent magnet flux linkages, stator inductance, and the number of pole pairs as design variables.

The stator flux linkages are computed from the equations

$$\varphi_d = L_d I_d + \sqrt{\frac{3}{2}}\varphi_{PM} \tag{17}$$

$$\varphi_q = L_q I_q \tag{18}$$

where φ_{PM} is permanent magnet flux linkage, φ_d and φ_q are stator flux linkages of the d-axis and q-axis, respectively, L_d and L_q are stator inductances of the d-axis and q-axis, respectively, and I_d and I_q are stator currents of the d-axis and q-axis, respectively. The toque and heat flow rates are then computed from

$$T = p(\varphi_d I_q - \varphi_q I_d) \tag{19}$$

$$dh = R_s I_d^2 + R_s I_q^2 \tag{20}$$

where T is torque, p is number of pole pairs, dh is heat flow rate, and R_s is stator resistance.

2.2.3 Gear Ratio Design and Other Parameters. For the rotary mechanical gear ratio, we use the equations

$$w_{motor} = G \cdot w_{axle} \tag{21}$$

$$T_{axle} = G \cdot T_{motor} \tag{22}$$

where w_{motor} is motor velocity, w_{axle} is axle velocity, T_{motor} is motor torque, and T_{axle} is axle torque. Range and MPGe are computed on the EPA highway fuel economy driving cycle, the standard way to compare EV performance in the market. Top-speed and acceleration are computed for straight line running. We set initial vehicle mass, dimensions, and drag coefficient based on Nissan Leaf specifications [7,16]. Battery and motor masses change depending on variable design values: battery mass (kg) = total number of cells ($n_s \times n_p$) × mass of a cell, where approximate mass of a cell in Nissan Leaf is 1.53 kg [15]; motor mass (kg) = 21.6 + 0.532 × motor power (kW) [17]. The relation of driving performance and the size of battery pack is nonlinear because larger battery mass diminishes driving performance while more battery capacity improves driving range [18].

2.2.4 EV Manufacturing Cost. Since our design variables are for battery and motor designs, battery pack cost and motor cost are variable costs in the EV manufacturing cost model. The remaining costs are considered fixed. Battery cost currently ranges from $300 to $600 per kWh; it is decreasing with time and is expected to reach $250 per kWh by 2020 [19,20]. We used $500/kWh as battery cost for the case study and performed a parametric study with respect to this cost parameter. For motor cost calculation, we used the cost model in Ref. [17]: motor cost ($) = 16 × motor power (kW) + 385. We assumed that fixed cost is $6000, resulting in a manufacturing cost for an EV with 24 kWh battery estimated as $12,000 and 80 kW motor estimated as $1665.

2.3 CS Location Network Model (Operations). In the operations model, we focused on DC fast-CSs for round trips between cities using highways. Two different types of DC fast-CS coverage are used in the study: *local path coverage*, a CS attribute in the consumer demand model; and *total flow coverage*, an objective of location modeling. Local path coverage is defined as the percentage of possible paths (i.e., shortest round trips from a city of residence to another city using the highway) a consumer can drive without running out of power using the CSs. For example, if a consumer lives in a city out of 19 cites in the target state and he can drive to all 18 cities using CSs, local path coverage for her city is 100%. We assume that consumers fully charge the EV in their home, drive to a destination with the shortest highway, then drive back home. If a battery runs out and there are DC fast-CSs on the way, they use DC fast-CSs; otherwise, they use other options such as level 1 or level 2 CSs. We assume that there are level 1 or 2 CSs in every city, but they are not suitable for trips between cities due to long charging time. For local path coverage, if the coverage is 100%, a consumer can drive from her city of residence to any other select city using only DC fast-CSs; if the coverage is 50%, a consumer can drive only 50% of the possible paths using DC fast-CSs, and he needs to use level 1 or 2 CSs for the other 50% of the possible paths. When the locations of CSs are decided, the local path coverage of each city will be different, because possible paths are different according to each city (origin) as shown in Fig. 4.

Total flow coverage is defined as the percentage of total traffic flows that can be recharged. Possible paths for total flow coverage are defined as combinations of paths from one city to another. For example, if there are 19 cities in the target state, the number of possible paths is $19 \times 18/2 = 171$. Since each possible path has different amounts of traffic flow, a path with more flow should have more relative weight on CS location decisions. Maximizing flow coverage is the overall desirable goal to decide the optimal locations of CSs.

However, a consumer cares about her vehicle recharge need rather than the total recharged flow volume, and only about local paths including her city of residence. This is why total flow coverage is used for optimal locations, while local path coverage is used in the consumer demand model. The demand model in Sec. 2.4 below predicts demand for each city based on local path coverage, then adds up the demands for all cities to estimate total demand in the region of interest.

2.3.1 Location Model. The location model for DC fast-CSs, f_{CS} in Eq. (9), is established using practices in geographical analysis. Hodgson first proposed the flow capturing location-allocation

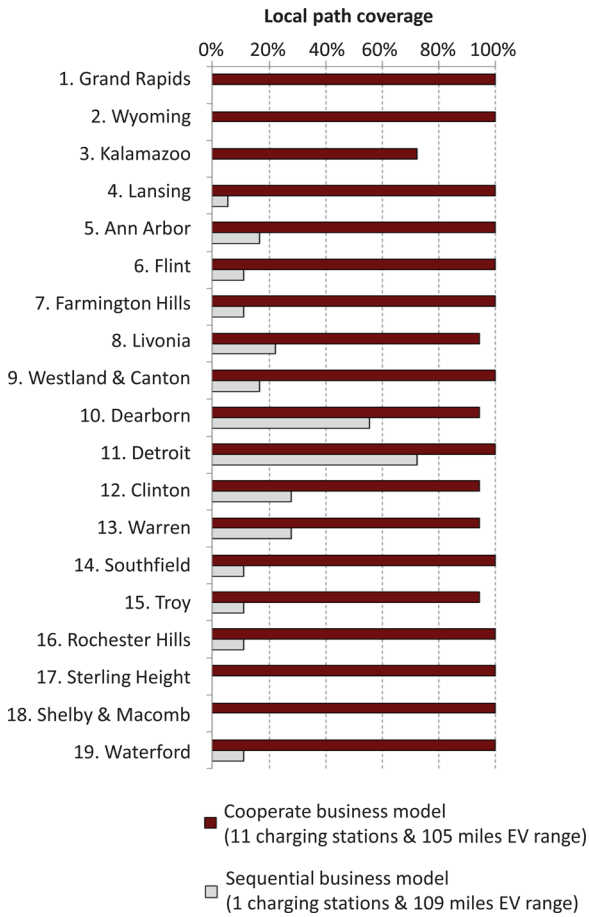

Fig. 4 CSs coverage for each city under two business models

model [21]. In this study, we adopt a model variant called the flow refueling location model (FRLM) [22–27] that has been widely used to find optimal locations of refueling facilities for alternative-fuel vehicles with limited range.

The standard FRLM [22] is used in the study resulting in a mixed-integer linear programming problem to maximize the flow coverage with respect to location of CSs given the number of stations and EV range

$$\max_{x,y,v} \quad \sum_{q\in Q} f_q y_q \tag{23}$$

subject to

$$\sum_{h\in H} b_{qh} v_h \geq y_q \quad \forall q \in Q \tag{24}$$

$$a_{hk} x_k \geq v_h \quad \forall h \in H; k \in K \tag{25}$$

$$\sum_{k\in K} x_k = p \tag{26}$$

$$x_k \in \{0,1\} \quad \forall k,h,q \tag{27}$$

$$0 \leq v_h \leq 1 \quad \forall h \tag{28}$$

$$0 \leq y_q \leq 1 \quad \forall q, \tag{29}$$

where q is the index of O–D pairs (O is an origin, D is a destination, and O–D pairs indicate the shortest paths for each pair); Q is the set of all O–D pairs; f_q is the flow volume on the shortest path between O–D pair q; $y_q = 1$ if f_q is captured, 0 otherwise; k is a potential station location; K is the set of all potential station locations; h is the index of combinations of stations; H is the set of all potential station combinations; $b_{qh} = 1$ if station combination h is open, 0 otherwise; $v_h = 1$ if all stations in combination h are open, 0 otherwise; $a_{hk} = 1$ if station k is in combination h, 0 otherwise; $x_k = 1$ if a station is located at k, 0 otherwise; and p is the number of stations to be located.

The objective function Eq. (23) maximizes the total flow volume (flow coverage % can also be used) that can be recharged with p stations. The flow between two cities, f_q, is calculated by a gravity model based on the city population and path distance (i.e., flow = population of city A × population of city B/path distance^2). In Eq. (24), at least one eligible combination of stations h should be open for path q to be recharged. In Eq. (25), v_h should be held to zero unless all stations k in combination h are open. In Eq. (26), p stations are required to be built. In Eq. (27), the CS location variables x_k are defined as binary variables. Although v_h and y_q are also defined as binary variables, they can be relaxed as continuous variables with lower and upper bounds in Eqs. (28) and (29), respectively. This trick can allow us to find an all-integer solution by reducing the number of required binary variables. More detailed explanation can be found in Ref. [22].

Before using the FRLM, we must pregenerate all combinations of stations, H, that can enable a path to be recharged following the six steps of [24]:

(1) Create the shortest path for all O–D pairs q and generate an empty master list of all station combinations h.
(2) Create a temporary list of all station combinations h of nodes on path q.
(3) Eliminate station combinations h that cannot recharge an EV on path q.
(4) Eliminate station combinations h if they include a subset that can recharge path q.
(5) Add it to the master list, if the list for path q still has any combination h:
Set $b_{qh} = 1$ if station combination h can recharge path q and 0 otherwise.
Set $a_{hk} = 1$ if station k is in station combination h and 0 otherwise.
(6) Reiterate steps 2–5 for all paths q.

Despite the stochastic nature of the genetic algorithm (GA), Lim and Kuby [26] reported being able to find global optima for network location problems. In the present study, we use GA to solve the location optimization problem with variables being the number of stations, station locations, and EV range; and output being the optimal flow coverage.

To reduce the computational cost for the integrated optimization problem of Fig. 1 (i.e., inner loop), while maintaining good model accuracy, we solved the station location problem (i.e., outer loop) offline. By varying the number of stations and EV range, we created a lookup table for optimal station locations encompassing all possible cases. Though, an EV's range is continuous, station coverage can be readily and accurately interpolated by using closely space, discrete range values; consequently, the integrated optimization problem can use the lookup table instead of the outer loop optimization, resulting in substantial computational cost reduction and high accuracy.

Figure 5 shows the optimal number and locations of CSs for the region of Southeast Michigan explained further in the case study below. Figure 6 shows how the local path coverage for Ann Arbor, MI, residents changes according to the number of CSs and EV range. More CSs and larger EV range typically result in larger local path coverage for each city. Since the optimal locations are decided to maximize total flow coverage not local path coverage for each city, small populated cities oftentimes are not served by this optimal locations. That is why local path coverage for Ann Arbor, MI in Fig. 6 sometimes decreases despite more CSs and larger EV range.

2.3.2 DC Fast-CS Operating Cost. The cost of DC fast-CS infrastructure can be decomposed into variable cost, such as electricity cost, and fixed cost such as installation, equipment, and maintenance cost. We use 10.28 cents per kWh as electricity cost based on average retail price for transportation in the U.S. for rolling 12-month period ending in January 2014 [28]. Fixed costs depend on the condition of stations. Here, we used $75,000 for installation and equipment cost, and $5500 for maintenance cost for 1 yr [29]. We evaluate profit and costs for CSs over a 10-yr period with discount rate 10% where the life cycle of EVs is assumed to be 10 yr.

2.4 Demand Model (Marketing). Demands for EV and CSs are predicted sequentially considering a heterogeneous market.

2.4.1 EV Demand. Hierarchical Bayesian (HB) choice-based conjoint [30,31] is used for building a heterogeneous EV demand model. Choice data are gathered using choice-based conjoint analysis. Individual-level discrete utility functions are estimated using the HB choice model. Spline curves are fitted to the individual-level posterior modes for each conjoint part-worth. Market demand is then calculated with choice probabilities based on individual-level utility functions and market potential.

The individual-level discrete utility v_{ij} is a linear function of discrete levels of attributes and defined as

$$v_{ij} = \sum_{k=1}^{K} \sum_{l=1}^{L_k} \beta_{ikl} z_{jkl} \tag{30}$$

where z_{jkl} are binary dummy variables indicating that alternative j possesses attribute k at level l, and β_{ikl} are the part-worth coefficients of attribute k at level l for individual i [32].

The HB choice model has two levels. At the upper level, an individual's part-worths, β_i, have a multivariate normal distribution, $\beta_i \sim N(\theta, \Lambda)$, where θ is a vector of means of the distribution of individuals and Λ is the covariance matrix of that distribution. At the lower level, choice probabilities for a logit model are used

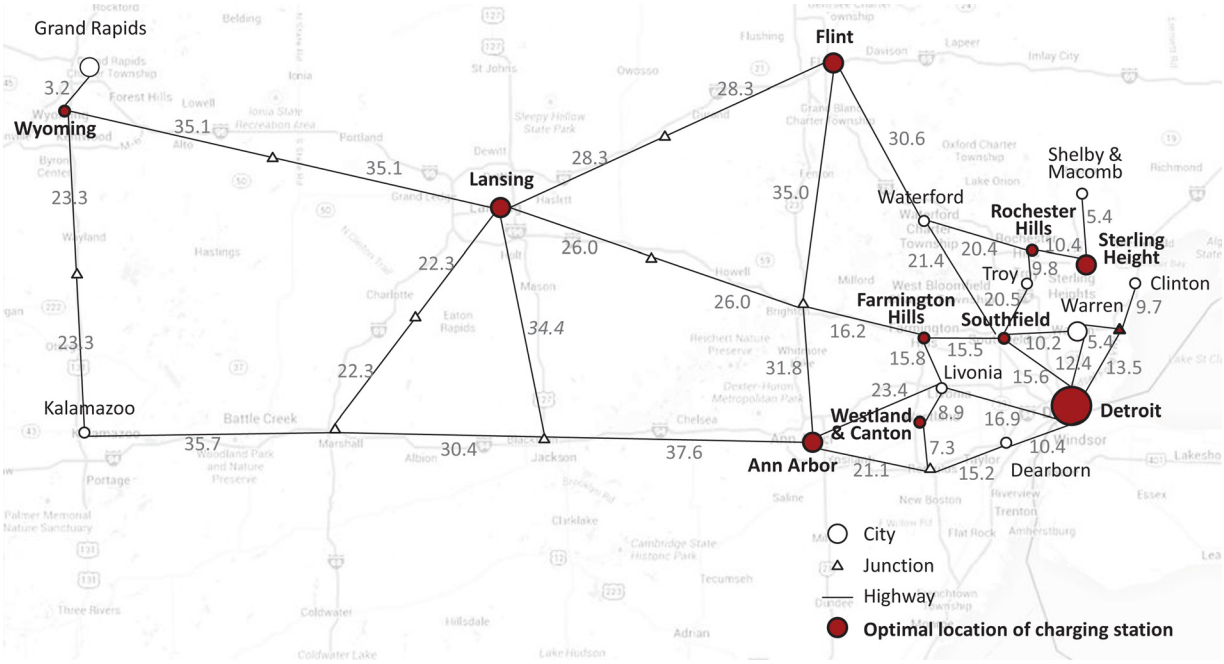

Fig. 5 Southeast Michigan highway network and optimal locations of CSs

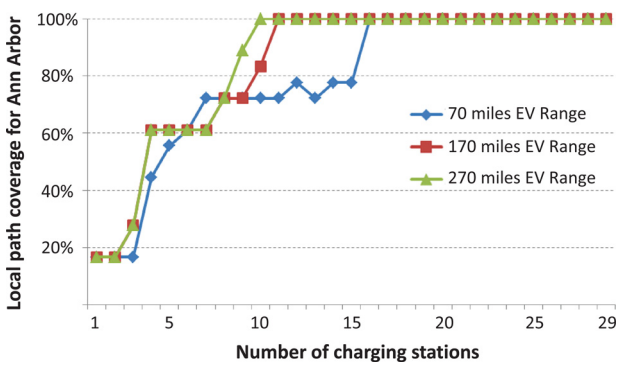

Fig. 6 Local path coverage of CSs for Ann Arbor, MI, residents

$$P_{ij} = \frac{e^{v_{ij}}}{\sum_{j' \in J} e^{v_{ij'}}} \tag{31}$$

where P_{ij} indicates that the probability individual i chooses option j from a set of alternatives J. Markov chain Monte Carlo (MCMC) is used to estimate the individual's part-worth. For the case study in Sec. 3, every tenth draw from the last 50,000 (of 100,000 total) draws were used to obtain the individual's parameter. The utility function in Eq. (30) based on the HB choice model cannot be used for continuous design decisions because the function is discrete. We calculate interpolated values of discrete part-worths using cubic splines so that choice probabilities for continuous design decisions can be estimated. To be specific about the actual procedure: We estimated 124 individual-level utility models, using 5000 draws each (via MCMC), assuming that part-worths follow a multivariate normal distribution across the 124 respondents; this is the standard assumption in such models, and is built, for example, into dedicated high-end conjoint software (e.g., Sawtooth [31]). We then interpolated each of the 124 subjects' part-worths to obtain a continuous design decision space in order to optimize profit; a similar procedure appeared in, for example, Michalek et al. [33].

Average market demand is calculated based on individual-level choice probabilities as

$$q_j = \frac{1}{I} \sum_{i=1}^{I} s P_{ij} \tag{32}$$

where q_j is market demand of option j, s is the potential market size, and I is total number of individuals. Note that this averaging of individual market demands is used only for optimization. When we compare demands of different design decisions, each individual-level market demand should be compared to account for heterogeneity. In this case, the comparison tells us what percentage of the individual market cases for one design decision is better than the other design decision as shown in Fig. 7. More detailed description of marketing demand models for design decisions can be found in Refs. [33] and [34].

EV demand is computed with Eq. (32) using the attributes and levels of EV and CSs shown in Table 3, selected based on previous research and the current EV market [35]. After building 124 individual-level utility models, we calculated the importances of attributes for each individual-level model, and then we averaged importances, as shown in Table 3. Demands for each city are computed first, then are summed up for total demand in the region, because local path coverage of CSs

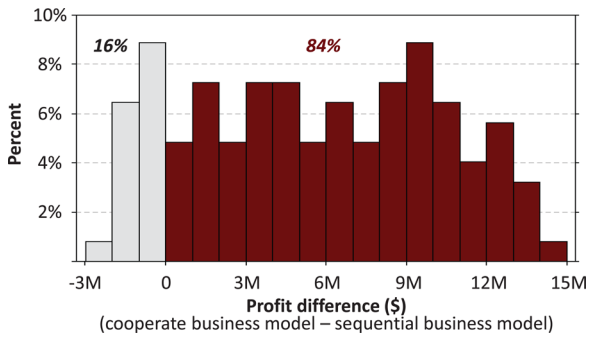

Fig. 7 Histogram of profit differences between results from the two business models

Table 3 Attribute levels and importance

Attributes	Unit	Level 1	2	3	4	5	Importance (%)
Local path coverage	%	0	25	50	75	100	27.2
Charging fee	$	0	2	5	8	10	13.7
Vehicle price	$	20 K	30 K	40 K	50 K	60 K	32.0
Range	miles	70	120	170	220	270	15.5
Fuel efficiency	MPGe	70	100	130	160	190	3.8
Top-speed	Mph	70	85	100	115	130	3.9
Acceleration (0–60 mph)	s	8	13	19	25	30	3.9

depends on each city location as explained in Sec. 2.3. The potential market sizes of each city are assumed according to population size so that local path coverage in a more populated city will have more influence on optimal decisions. Charging fee ($) is the battery 80% capacity charging fee. For easy comparison with a gasoline vehicle, the average gas price in MI ($3.776 per gallon on April 6, 2014 [36]) was provided in the conjoint survey.

2.4.2 DC Fast-CS Demand. Public DC fast-CS demands for each city are estimated sequentially based on EV demand. This is because EV drivers are potential consumers of CSs during the EV and CS life cycles. Many scenarios of charging behavior can be considered [37]. Here, we estimate charging events based on observed data of EV users from a particular EV project [6,38], which showed that the mean number of charging events per vehicle-day driven is 1.05, and approximately 4.64% of charging events is from public DC fast-CSs. We predict CS demand over 10 yr to evaluate profitability of the infrastructure investment. A parametric study on the impact of these assumed parameter values is included in the discussion below.

3 Case Study: Southeast Michigan Market

The proposed decision-making framework is applied on the potential EV market in Southeast Michigan. In the operations model, the relevant portion of Michigan's highway network used to determine possible paths and flows is shown in Fig. 5. There are no public DC fast-CSs in Michigan at the time of this writing. A total of 29 locations (19 cities and ten junctions) are selected as candidates for CS locations. Nineteen cities are selected based on their population, with some neighboring cities grouped and treated as a single one. Circle nodes indicate cities where CSs exist, size of circles represents the size of population, lines indicate shortest highway paths, numbers indicate path distances between nodes, and triangles indicate additional junctions needed for CSs because of limited EV range.

For the marketing demand model, 124 subjects who live in Southeast Michigan were engaged through ClearVoice Research [39] and surveyed on-line using SAWTOOTH software [31]. The subjects consisted of 40% males and 60% females; 3% were 18–24 yr of age, 20% were 25–34 yr of age, 22% were 35–44 yr of age, 14% were 45–54 yr of age, 26% were 55–64 yr of age, and 15% were more than 65 yr of age. Table 3 shows the average relative importance of the attributes in the model based on estimated part-worths of attribute levels. The CS coverage and vehicle price are evidently important in consumer choices. The total 2014 U.S. EV sales can be projected to 76,820 because it is predicted that EV sales will increase by 67% in 2014 compared to 2013 [40,41]. We assume that the potential EV market size depends on population size. Since the population of the targeted 19 cities in SE Michigan makes up 0.85% of the U.S. population [42], the potential EV market size of Southeast Michigan was assumed to be 656 in this study. Then, potential market sizes for each city were assigned based on city population size. We considered only other EVs (i.e., the newly designed EV versus existing EV vehicles). Two EV competitors operating in Michigan were assumed in computing market share so that the sum of demands of three manufactures and no choice makes 100%.

Table 4 Optimal decision values

Model	Variable	Optimal value
Marketing	Vehicle price	$44,211
	Charging fee	$4.0
Engineering	Number of cells in series in one branch	164
	Number of branches in parallel	1
	Stator inductance of the *d*-axis	1.80 mH
	Stator inductance of the *q*-axis	2.21 mH
	Stator resistance	0.052 Ω
	Number of pole pairs	3
	Gear ratio	3.87
Operations	Number of stations (out of 29 candidates)	11
	Stations locations	See Fig. 5

Table 5 Responses of two business models

		Cooperative business model	Sequential business model
Market response	Total profit	$8.39 M	$2.80 M
	EV profit	$9.52 M	$2.78 M
	Station profit	−$1.13 M	$0.02 M
	Market share	55.8%	20.0%
EV attributes and specs	Vehicle price	$44,211	$40,208
	Range	105.2 miles	108.9 miles
	Top-speed	117.8 mph	119.2 mph
	Acceleration	13.2 s	12.3 s
	MPGe	172.0	166.8
	Battery capacity	20.6 kWh	22.0 kWh
	Motor power	93.3 kW	99.6 kW
EV cost	Battery cost	$10,314	$11,006
	Motor cost	$1879	$1978
CS attributes	Charging fee	$4.0	$10.0
	Number of stations	11	1 (Detroit)
	Local path coverage (average of 19 cities)	97.1%	16.4%
CS cost	Installation and equipment	$825,000	$75,000
	Maintenance (10 yr)	$371,746	$33,795

Note: Market response shown in this table is the mean of market response distribution.

MATLAB's implementation of the GA algorithm [43] was used to solve the mixed-integer optimization problem of Eq. (1). We executed three parallel runs with different initial guesses.[2] The best result is reported in this study. The results were very close giving some assurance of GA convergence. The computed optimal decision values are summarized in Table 4. Response values for these optimal decision values are shown in the left-hand column (cooperative business model) in Table 5. Note that market responses correspond to the average values of 124 market scenarios using individual-level demand models. Since we considered a heterogeneous market in demand modeling, market response is represented by the distribution of individual responses. The results indicate that the CS operator must build eleven stations (out of 29 candidates) located in ten cities (i.e., Wyoming, Lansing, Ann Arbor, Flint, Farmington hills, Westland & Canton, Detroit, Southfield, Rochester hills, and Sterling height) and in one junction between

[2]On an Intel i7 CPU 860@2.80 GHz and 8.00 GB RAM, an optimization run took 36 hr on average.

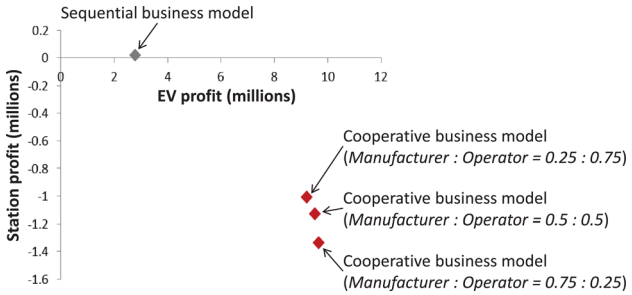

Fig. 8 Tradeoff between EV profit and station profit

Warren and Clinton, see Fig. 5. CS local path coverages for 19 cities are shown in Fig. 4.

4 Discussion

Two different business models are compared in order to determine the value of the cooperative business model, described so far. The cooperative business model considers EV manufacturer and fast-CS operator as a single decision entity and finds optimal decisions for EV and stations simultaneously by maximizing overall profit (i.e., EV profit + CS profit). For this business model, EV manufacturers are encouraged to expand their business to CS operations or partner with existing utilities or CS manufacturers, sharing profit and loss.

The second business model is a "sequential" model similar to current practice, where the EV OEM designs EVs to maximize OEM profit, and the CS provider makes location decisions for given EV designs to maximize operation profit.

Results for these two business models are compared in Table 5. It is shown that the cooperative model brings higher overall profit and market share than the sequential model, where market responses are average values of 124 responses based on the individual demand models. For comparison of heterogeneous market scenarios, we examined 124 responses as shown in Fig. 7, so that 84% of responses shows that the cooperative business model offers more profit than the sequential one (i.e., positive difference).

The cooperative model requires relatively lower EV performance in range, top-speed, acceleration, battery capacity, and motor power than the sequential one, even if the vehicle price is higher. Regarding CS attributes, the sequential model could not build enough CSs (i.e., one station for Detroit and 16.4% coverage) and offered higher charging fee than the cooperative model.

One may conclude that, under the modeling assumptions made, a noncooperative business model does not improve the attractiveness of EVs to consumers. While the sparse CS infrastructure of the sequential model can be the main reason of range anxiety, a balance between EV performance and CS infrastructure can effectively reduce consumer range anxiety. The cooperative model allows for more market share by supplying low charging fee and larger CS coverage to consumers despite lower performance and higher vehicle price than the sequential model. Since the cooperative model allows negative profit of CSs, attractive CS attributes can boost EV adoption share, resulting in higher overall profit than the sum of the two positive individual profits from EV and CSs in the sequential model. This is an example of examining a product-service system in an integrated business model [44].

Typically, the nature of cooperation (i.e., sequential business model) is that an EV manufacturer or government provides some degree of financial support to a station provider within the target region. For example, regarding the recent news about the partnership between Toyota and California, the state plans to build hydrogen fuel stations for Toyota's fuel-cell-powered vehicle, the "Mirai," with subsidies from Toyota [45]. When station providers are public and receive subsidies from the manufacturer, even small or zero profit would be acceptable. In such situations, separate organizations can work together for the common goal of promoting an eco-friendly car market.

For simplicity, our objective function was the sum of profits, which could be taken to reflect an equal profit-sharing arrangement, i.e., 50–50%. To get a sense of what such a Pareto curve might look like, we resolved the multi-objective problem for two additional scenarios (i.e., ratios of EV manufacturer profit to CS operator profit of 75–25% and vice versa) as shown in Fig. 8. A complete Pareto curve can be generated by optimizing with different weightings on the unit interval.

Parametric studies for different battery cost parameters and for different charging behaviors (i.e., % of DC fast-CS events out of all charging events) were examined in a postoptimal analysis. The parametric study in Fig. 9 shows that when battery cost decreases from \$500 to \$200, optimal profit can increase by 31% with optimal 114 EV range. Similarly, when the DC charging event (%) increases by 1%, the profit increases by 0.25%. In addition, electricity costs are hard to predict over a 10-year business span, so to directly address these concerns we performed additional sensitivity analysis. We checked electricity prices in the target area (Michigan) over the last 5 yr [46] and found that nearly all variation was contained within one cent per kWh on either side of the value used here; consequently, we redid the entire analysis for a 1 cent increase and for a 1 cent decrease. The analysis suggests that a 1 cent deviation in electricity costs (per kWh) translates into 0.13% in profit change. This may appear as if profit is relatively insensitive to even sizable increases in electricity costs. However, one must bear in mind that the chief costs of CSs are construction and maintenance, as opposed to electricity itself.

There are several limitations and avenues for future work. First, the local path coverage attribute used in the conjoint survey could

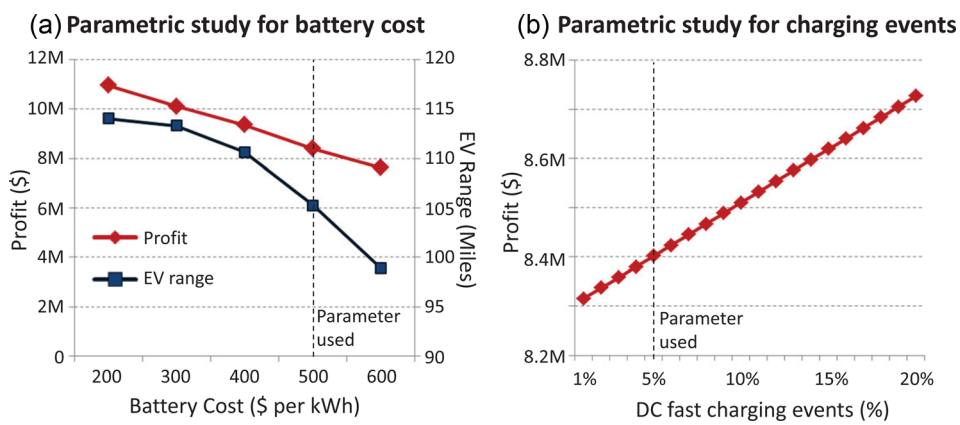

Fig. 9 Postoptimal analysis

be somewhat abstract for respondents. We did anticipate this and, before presenting respondents with the conjoint survey, we asked them to assume that: they will use only the highway; the origin is their home city; and the destinations are other cities. So, local path coverage means how many cities they can drive to from their home city without running out of battery power. In a future study, we plan to examine which representation(s) of the station coverage attribute is most appropriate or evocative for conjoint surveys.

Second, our framework assumed an "exclusive" channel between manufacturer and operator, so that the station operator does not supply charging services to other manufacturers. Other work [47] has addressed "nonexclusive" channels between products and services (in the tablet and E-service market, specifically) and proposed a service demand model via conditional probability given product choice. The framework here can be adapted to using this service demand model under a nonexclusive channel structure.

Third, this study used a single vehicle type, in order to keep the presentation focused. The general framework can readily be expanded to multiple vehicle types for product line design, e.g., [33]. Future research will consider different vehicle architectures, including plug-in hybrid electric vehicle as well as battery electric vehicle, but much more substantive detail would be required to broach such issues here.

Finally, we did not consider the "capacity and queuing problem" for CSs, for a specific reason: our assumption is that consumers recharge vehicles fully at home before driving and can use level 1 or 2 CSs, as well as fast DC CSs, during their daily or even longer travels. Future research will consider this issue by adopting the advanced FRLM model [25].

5 Conclusion

The proposed integrated decision-making framework allows quantification of the tradeoffs among various business models for the EV market. A cooperative business model presents more advantages than the existing noncooperative business model. The results clearly depend on the modeling assumptions made; however, these are generally sufficiently plausible to support the case for a cooperative approach to improve consumer adoption of EVs.

In future work, a government policy model can be integrated in the proposed framework to explore quantitatively how government incentives and regulations can affect market decisions.

Acknowledgment

This research was partially supported by a Graham Institute Doctoral Fellowship at the University of Michigan. This support was gratefully acknowledged.

Nomenclature

Profit Optimization and Demand Models (Marketing)

c_{CS} = CS operating cost
c_{EC} = electricity cost
c_{EV} = EV manufacturing cost
p_{CS} = charging fee
p_{EV} = EV price
q_{CS} = CS demand
q_{EV} = EV demand
Π_{CS} = charging station (CS) profit
Π_{EV} = electric vehicle (EV) profit

EV Design Model (Engineering)

$\mathbf{A}_{EV}$ = EV attributes
acc_{EV} = acceleration
$\mathbf{B}_{EV}$ = battery design variables
G_{EV} = gear ratio
$\mathbf{M}_{EV}$ = motor design variables
mpg_{EV} = miles per gallon gasoline equivalent
r_{EV} = range
sp_{EV} = top-speed
$\mathbf{x}_{EV}$ = EV design variables

CS Location Network Model (Operations)

$\mathbf{CV}_{CS}$ = CS coverage of target locations
$\mathbf{L}_{CS}$ = CS locations
N_{CS} = number of CS
$\mathbf{x}_{CS}$ = CS design variables

References

[1] Vardera, L., 2010, *The Electric Vehicle Market in the USA*, Market Report, Finpro, Stamford, CT.
[2] Egbue, O., and Long, S., 2012, "Barriers to Widespread Adoption of Electric Vehicles: An Analysis of Consumer Attitudes and Perceptions," Energy Policy, **48**, pp. 717–729.
[3] Kley, F., Lerch, C., and Dallinger, D., 2011, "New Business Models for Electric Cars-A Holistic Approach," Energy Policy, **39**(6), pp. 3392–3403.
[4] Melaina, M., and Bremson, J., 2008, "Refueling Availability for Alternative Fuel Vehicle Markets: Sufficient Urban Station Coverage," Energy Policy, **36**, pp. 3233–3241.
[5] Pearre, N., Kempton, W., Guensler, R., and Elango, V., 2011, "Electric Vehicles: How Much Range Is Required for a Days Driving?," Transp. Res. Part C: Emerging Technol., **19**(6), pp. 1171–1184.
[6] Smart, J., and Schey, S., 2012, "Battery Electric Vehicle Driving and Charging Behavior Observed Early in the EV Project," SAE Int. J. Altern. Powertrains, **1**(1), pp. 27–33.
[7] Wikipedia, 2014, "Nissan Leaf." Available at: http://en.wikipedia.org
[8] ECOtality, 2014, "The EV Project." Available at: http://www.theevproject.com
[9] ChargePoint, 2014, "Charge Point." Available at: http://www.chargepoint.com
[10] Young, A., 2014, "Number of Electric Car Fast Charge Stations." Available at: http://www.ibtimes.com
[11] AMESim, 2014." Available at: http://www.lmsintl.com
[12] Chan, H., 2000, "A New Battery Model for Use With Battery Energy Storage Systems and Electric Vehicles Power Systems," Power Engineering Society Winter Meeting, Vol. 1, IEEE, pp. 470–475.
[13] Lee, S., and Tolbert, L., 2009, "Analytical Method of Torque Calculation for Interior Permanent Magnet Synchronous Machines," Energy Conversion Congress and Exposition, IEEE, pp. 173–177.
[14] Tenner, S., Gunther, S., and Hofmann, W., 2011, "Loss Minimization of Electric Drive Systems Using a DC/DC Converter and an Optimized Battery Voltage in Automotive Applications," Vehicle Power and Propulsion Conference (VPPC), IEEE, pp. 1–7.
[15] INL, 2011, "2011 Nissan Leaf – VIN 0356 – Advanced Vehicle Testing—Beginning of Test Battery Testing Results," Advanced Vehicle Testing Activity, Idaho National Laboratory (INL).
[16] INL, 2011, "2011 Nissan Leaf—VIN 0356 – Advanced Vehicle Testing—Baseline Testing Results," Advanced Vehicle Testing Activity, Idaho National Laboratory (INL).
[17] Simpson, A., 2006, "Cost-Benefit Analysis of Plug-In Hybrid Electric Vehicle Technology," 22nd International Battery, Hybrid and Fuel Cell Electric Vehicle Symposium and Exhibition, National Renewable Energy Laboratory, pp. 1–12.
[18] Karabasoglu, O., and Michalek, J., 2013, "Influence of Driving Patterns on Life Cycle Cost and Emissions of Hybrid and Plug-In Electric Vehicle Powertrains," Energy Policy, **60**, pp. 445–461.
[19] Traut, E., Hendrickson, C., Klampfl, E., Liu, Y., and Michalek, J., 2012, "Optimal Design and Allocation of Electrified Vehicles and Dedicated Charging Infrastructure for Minimum Life Cycle Greenhouse Gas Emissions and Cost," Energy Policy, **51**, pp. 524–534.
[20] Henry, L., and Lovellette, G., 2011, "Will Electric Cars Transform the U.S. Vehicle Market?," Belfer Center for Science and International Affairs, Harvard Kennedy School, Discussion Paper No. 2011-08.
[21] Hodgson, M., 1990, "A Flow-Capturing Location-Allocation Model," Geogr. Anal., **22**(3), pp. 270–279.
[22] Kuby, M., and Lim, S., 2005, "The Flow-Refueling Location Problem for Alternative-Fuel Vehicles," Socio-Econ. Plann. Sci., **39**(2), pp. 125–145.
[23] Kuby, M., Lim, S., and Upchurch, C., 2005, "Dispersion of Nodes Added to a Network," Geogr. Anal., **37**(4), pp. 383–409.
[24] Kuby, M., and Lim, S., 2007, "Location of Alternative-Fuel Stations Using the Flow-Refueling Location Model and Dispersion of Candidate Sites on Arcs," Networks Spat. Econ., **7**(2), pp. 129–152.
[25] Upchurch, C., Kuby, M., and Lim, S., 2009, "A Model for Location of Capacitated Alternative-Fuel Stations," Geogr. Anal., **41**(1), pp. 85–106.
[26] Lim, S., and Kuby, M., 2010, "Heuristic Algorithms for Siting Alternative-Fuel Stations Using the Flow-Refueling Location Model," Eur. J. Oper. Res., **204**(1), pp. 51–61.
[27] Kim, J., and Kuby, M., 2012, "The Deviation-Flow Refueling Location Model for Optimizing a Network of Refueling Stations," Int. J. Hydrogen Energy, **37**(6), pp. 5406–5420.
[28] EIA, 2014, "Electric Power Monthly With Data for January 2014, Energy Information Administration (EIA), Washington, DC.

[29] Schroeder, A., and Traber, T., 2012, "The Economics of Fast Charging Infrastructure for Electric Vehicles," Energy Policy, **43**, pp. 136–144.
[30] Rossi, P., Allenby, G., and McCulloch, R., 2005, *Bayesian Statistics and Marketing*, Wiley, Hoboken, NJ.
[31] Orme, B., 2009, "The CBC/HB System for Hierarchical Bayes Estimation Version 5.0 Technical Paper," Technical Paper Series, Sawtooth Software, Orem, UT.
[32] Green, P., and Krieger, A., 1996, "Individualized Hybrid Models for Conjoint Analysis," Manage. Sci., **42**(6), pp. 850–867.
[33] Michalek, J. J., Ebbes, P., Adigüzel, F., Feinberg, F. M., and Papalambros, P. Y., 2011, "Enhancing Marketing With Engineering: Optimal Product Line Design for Heterogeneous Markets," Int. J. Res. Mark., **28**(1), pp. 1–12.
[34] Chen, W., Hoyle, C., and Wassenaar, H., 2012, *Decision-Based Design: Integrating Consumer Preferences into Engineering Design*, Springer, London.
[35] Hidrue, M., Parsons, G., Kempton, W., and Gardner, M., 2011, "Willingness to Pay for Electric Vehicles and Their Attributes," Resour. Energy Econ., **33**(3), pp. 686–705.
[36] GasBuddy, 2014, "Michigan Gas Price." Available at: http://www.michigangasprices.com
[37] Peterson, S., and Michalek, J., 2012, "Cost-Effectiveness of Plug-In Hybrid Electric Vehicle Battery Capacity and Charging Infrastructure Investment for Reducing U.S. Gasoline Consumption," Energy Policy, **52**, pp. 429–438.
[38] ECOtality, 2013, "Q2 2013 Report—The EV Project. Electric Transportation Engineering Corporation," ECOtality North America, Phoenix, AZ, Quarterly Report No. INL/MIS-10-19479.
[39] Clearvoice, 2014, "Clearvoice Research." Available at: http://www.clearvoiceresearch.com
[40] Loveday, E., 2014, "BEV Sales in U.S. in 2013." Available at: http://insideevs.com
[41] IHS, 2014, "Global Production of Electric Vehicles to Surge by 67 Percent This Year," http://press.ihs.com
[42] Census, 2014, "2010 United States Census." Available at: http://www.census.gov
[43] MathWorks, 2014, "MATLAB r2013a." Available at: http://www.mathworks.com
[44] Kang, N., Feinberg, F. M., and Papalambros, P. Y., 2013, "A Framework for Enterprise-Driven Product Service Systems Design," 19th International Conference on Engineering Design (ICED13), Seoul, Korea, Aug. 19–22, pp. 297–308.
[45] Lippert, J., 2014, "Toyota Plans Mirai Fuel-Cell Car Traveling 300 Miles Per Tank," http://www.bloomberg.com
[46] Bureau of Labor Statistics, 2014, "Average Energy Prices," Detroit-Ann Arbor-Flint, http://www.bls.gov
[47] Kang, N., 2014, "Multidomain Demand Modeling in Design for Market Systems," Ph.D. thesis, University of Michigan, Ann Arbor, MI.